PERFORMANCE ANALYSIS OF COARRAY-BASED MUSIC AND THE CRAMÉR-RAO BOUND

Mianzhi Wang, Zhen Zhang, and Arye Nehorai

Preston M. Green Department of Electrical and Systems Engineering
Washington University in St. Louis, USA

ABSTRACT

Sparse linear arrays, such as co-prime and nested arrays, can identify up to $\mathcal{O}(M^2)$ sources with only $\mathcal{O}(M)$ sensors by using co-array based MUSIC. We conduct analytical performance analysis of two coarray based MUSIC algorithms, namely the direct augmentation based MUSIC, and the spatial smoothing based MUSIC. In addition, we analyze the Cramér-Rao bound for sparse linear arrays, and show that for co-prime and nested arrays, it can decrease at a rate of $\mathcal{O}(M^{-5})$ as the number of sensors M goes to infinity, in contrast to $\mathcal{O}(M^{-3})$ in the ULA case. We use numerical examples to demonstrate our analytical results.

***Index Terms*—** performance analysis, mean-square error, MUSIC, sparse linear arrays, Cramer-Rao bound

1. INTRODUCTION

Recently, new types of sparse linear arrays have been proposed, such as co-prime arrays [1–3] and nested arrays [4–6]. Unlike uniform linear arrays (ULAs), these arrays have the attractive property of providing up to $\mathcal{O}(M^2)$ degrees of freedom with only M sensors, which is possible by exploiting the so-called coarray structure. An augmented (coarray) covariance matrix with dimension $\mathcal{O}(M^2)$ can then be constructed, and MUSIC [7] can be applied to identify up to $\mathcal{O}(M^2)$ sources. We call the MUSIC algorithm applied to the coarray covariance matrix "coarray-based MUSIC," to distinguish it from the MUSIC algorithm directly applied to the original sample covariance matrix.

In [8] and [9], the authors conducted a detailed analysis of the performance of the MUSIC estimator. They derived the asymptotic mean-square error (MSE) expression of the MUSIC estimator and rigorously analyzed its statistical efficiency. Later in [10], the authors derived a unified mean-square error (MSE) expression for various subspace-based estimators based on first-order perturbation theory. However, because the coarray covariance matrix has different statistical properties from the original sample covariance matrix, these results cannot be applied to coarray-based MUSIC. In [11], the authors first derived a general asymptotic MSE expression for the MUSIC algorithm applied to matrices transformed from the sample covariance matrix. While this expression is applicable to coarray-based MUSIC, its explicit form is very complicated. In this paper, we present a simpler and more revealing asymptotic MSE expression for two commonly used coarray-based MUSIC algorithms. Additionally, we numerically show that our asymptotic MSE expression can well predict the resolution limit of coarray-based MUSIC.

The Cramér-Rao bound (CRB) for uniform linear arrays was well-investigated in [8, 9]. Recently, in [12–15], the authors independently derived the CRB for sparse linear arrays in the case when the number of sources exceeds the number of sensors. In this paper, we further investigate how the CRB various according to the number of sensors. We show that for co-prime and nested arrays, the Cramér-Rao bound (CRB) can decrease at a rate of $\mathcal{O}(M^{-5})$ as $M \to \infty$.

2. THE COARRAY-BASED MUSIC

We consider an M-sensor sparse linear array whose sensors are located on a uniform grid. The sensor locations are given by $\mathcal{D} = \{d_1, d_2, \ldots, d_M\}$. We also denote the sensor locations using the integer set $\bar{\mathcal{D}} = \{\bar{d}_1, \bar{d}_2, \ldots, \bar{d}_M\}$, where $\bar{d}_i = d_i/d_0$ for $i = 1, 2, \ldots, M$, and d_0 is the grid size. Examples of such sparse linear arrays include co-prime and nested arrays, whose definitions are given in Definition 1.

Definition 1. *A co-prime array generated by the co-prime pair (M, N) is given by $\{0, M, \ldots, (N-1)M\} \cup \{N, 2N, \ldots, (2M-1)N\}$ [1]. A nested array generated by the parameter pair (N_1, N_2) is given by $\{0, 1, \ldots, N_1 - 1\} \cup \{N_1, 2N_1 + 1, \ldots, N_2N_1 + N_2 - 1\}$ [4].*

We assume K far-field narrow-band sources impinging on the array from directions $\theta_1, \theta_2, \ldots, \theta_K$. The received measurement vectors can be expressed as

$$\boldsymbol{y}(t) = \boldsymbol{A}(\theta)\boldsymbol{x}(t) + \boldsymbol{n}(t), t = 1, 2, \ldots, N, \qquad (1)$$

where $\boldsymbol{A} = [\boldsymbol{a}(\theta_1)\, \boldsymbol{a}(\theta_2)\, \ldots\, \boldsymbol{a}(\theta_K)]$ denotes the array steering matrix, $\boldsymbol{x}(t)$ denotes the source signal vector, $\boldsymbol{n}(t)$ denotes additive complex white Gaussian noise, and N denotes the number of snapshots. We adopt the unconditional

This work was supported by the ONR Grant N000141310050.

model in [16] which assumes that $x(t)$ follows the circularly-symmetric Gaussian complex Gaussian distribution. We assume that the sources are uncorrelated and that the additive noise is uncorrelated from the sources. We further assume no temporal correlation between each snapshot.

Under the aforementioned assumptions, the sample covariance matrix is given by $\boldsymbol{R} = \boldsymbol{A}\boldsymbol{P}\boldsymbol{A}^H + \sigma_{\mathrm{n}}^2\boldsymbol{I}$, where $\boldsymbol{P} = \mathrm{diag}(p_1, p_2, \ldots, p_K)$, p_k is the power of the k-th source, and σ_{n}^2 denotes the variance of the additive noise. By vectorizing $\boldsymbol{R}$, we obtain

$$\boldsymbol{r} = \boldsymbol{A}_{\mathrm{d}}\boldsymbol{p} + \sigma_{\mathrm{n}}^2\boldsymbol{i}, \tag{2}$$

where $\boldsymbol{A}_{\mathrm{d}} = \boldsymbol{A}^* \odot \boldsymbol{A}$, $\odot$ denotes the Khatri-Rao product [17], $\boldsymbol{p} = [p_1, p_2, \ldots, p_K]^T$, $\boldsymbol{i} = \mathrm{vec}(\boldsymbol{I})$. For a matrix $\boldsymbol{A} = [\boldsymbol{a}_1\ \boldsymbol{a}_2\ \ldots\ \boldsymbol{a}_N]$, we define $\mathrm{vec}(\boldsymbol{A}) = [\boldsymbol{a}_1^T\ \boldsymbol{a}_2^T\ \ldots\ \boldsymbol{a}_N^T]^T$

We can observe that $\boldsymbol{A}_{\mathrm{d}}$ embeds a steering matrix of an array whose sensor locations are given by $\mathcal{D}_{\mathrm{co}} = \{d_m - d_n | 1 \le m, n \le M\}$. By averaging the redundant rows of $\boldsymbol{A}_{\mathrm{d}}$, we can construct a new steering matrix representing a virtual ULA with enhanced degrees of freedom. It can be easily shown that this virtual ULA is centered at the origin. Therefore we can denote its sensor locations by $[-M_{\mathrm{v}}+1, -M_{\mathrm{v}}+2, \ldots, 0, \ldots, M_{\mathrm{v}}-1]d_0$, where M_{v} is defined such that $2M_{\mathrm{v}}-1$ is the size of the virtual ULA. To better illustrate the relationship between the physical array model and the coarray model, we introduce the following definitions.

Definition 2. *The array weight function [4] $\omega(n) : \mathbb{Z} \mapsto \mathbb{Z}$ is defined by $\omega(l) = |\{(m,n)|\bar{d}_m - \bar{d}_n = l\}|$, where $|\mathcal{A}|$ denote the cardinality of the set $\mathcal{A}$.*

Definition 3. *The transform matrix [12] $\boldsymbol{F}$ is a real matrix of size $(2M_{\mathrm{v}}-1) \times M^2$, whose elements are defined by*

$$F_{m,p+(q-1)M} = \begin{cases} \frac{1}{\omega(m-M_{\mathrm{v}})} & ,\bar{d}_p - \bar{d}_q = m - M_{\mathrm{v}}, \\ 0 & ,\mathrm{otherwise}, \end{cases} \tag{3}$$

for $m = 1, 2, \ldots, M_{\mathrm{v}}, p = 1, 2, \ldots, M, q = 1, 2, \ldots, M$.

Base on these definitions, we can express the measurement vector of the virtual ULA by $\boldsymbol{z} = \boldsymbol{F}\boldsymbol{r} = \boldsymbol{A}_{\mathrm{c}}\boldsymbol{p} + \sigma_{\mathrm{n}}^2\boldsymbol{F}\boldsymbol{i}$, where $\boldsymbol{A}_{\mathrm{c}}$ represents the steering matrix of the virtual ULA, and $\boldsymbol{i} = \mathrm{vec}(\boldsymbol{I})$. The virtual ULA can be divided into M_{v} overlapping uniform subarrays of size M_{v}, whose outputs are given by $\boldsymbol{z}_i = \boldsymbol{\Gamma}_i\boldsymbol{z}$ for $i = 1, 2, \ldots, M_{\mathrm{v}}$. $\boldsymbol{\Gamma}_i = [\boldsymbol{0}_{M_{\mathrm{v}}\times(i-1)}\ \boldsymbol{I}_{M_{\mathrm{v}}\times M_{\mathrm{v}}}\ \boldsymbol{0}_{M_{\mathrm{v}}\times(M_{\mathrm{v}}-i)}]$ represents the selection matrix for the i-th subarray. Given $\boldsymbol{z}_i$, two common ways of constructing $\boldsymbol{R}_{\mathrm{v}}$ can be expressed as:

$$\boldsymbol{R}_{\mathrm{v}1} = [\boldsymbol{z}_{M_{\mathrm{v}}}\ \boldsymbol{z}_{M_{\mathrm{v}}-1}\ \cdots\ \boldsymbol{z}_1], \tag{4a}$$

$$\boldsymbol{R}_{\mathrm{v}2} = \frac{1}{M_{\mathrm{v}}}\sum_{i=1}^{M_{\mathrm{v}}} \boldsymbol{z}_i\boldsymbol{z}_i^H. \tag{4b}$$

Method (4a) corresponds to the direct augmentation approach [18, 19], while method (4b) corresponds to the rank enhanced spatial smoothing approach introduced in [4]. For brevity, we use the term "direct augmentation based MUSIC" (DA-MUSIC) and the term "spatial smoothing based MUSIC" (SS-MUSIC) to denote the MUSIC algorithm applied to $\boldsymbol{R}_{\mathrm{v}1}$ and $\boldsymbol{R}_{\mathrm{v}2}$, respectively. If we design a sparse linear array such that $M_{\mathrm{v}} > M$, both DA-MUSIC and SS-MUSIC can identify more sources than M.

We observe from (4a) and (4b) that $\boldsymbol{R}_{\mathrm{v}1}$ and $\boldsymbol{R}_{\mathrm{v}2}$ have different statistical properties from $\boldsymbol{R}$. Therefore the asymptotic MSE expression for the classical MUSIC algorithm does not work for coarray-based MUSIC. We will present the new asymptotic MSE expression in the following section.

3. THE MEAN-SQUARE ERROR

Note that both $\boldsymbol{R}_{\mathrm{v}1}$ and $\boldsymbol{R}_{\mathrm{v}2}$ are constructed from $\boldsymbol{R}$. However, in practice, the real sample covariance matrix $\boldsymbol{R}$ is unobtainable, and its maximum-likelihood estimate $\hat{\boldsymbol{R}} = \frac{1}{N}\sum_{t=1}^{N}\boldsymbol{x}(t)\boldsymbol{x}(t)^H$ is used. The estimated signal subspace does not accurately represent the true signal subspace, leading to DOA estimation errors. The perturbation of the signal subspace can be attributed to the estimation error $\Delta\boldsymbol{R} = \hat{\boldsymbol{R}} - \boldsymbol{R}$. Given a sufficient number of snapshots, the $\Delta\boldsymbol{R}$ will be sufficiently small, and we can analyze the asymptotic estimation errors of both DA-MUSIC and SS-MUSIC with eigenvector perturbation theory [20,21]. Our main results are summarized in Theorem 1 and Theorem 2 [12].

Theorem 1. *Let $\hat{\theta}_k^{(\mathrm{DA})}$ and $\hat{\theta}_k^{(\mathrm{SS})}$ denote the estimated values of θ_k using DA-MUSIC and SS-MUSIC, respectively. Let $\Delta\boldsymbol{r} = \mathrm{vec}(\hat{\boldsymbol{R}} - \boldsymbol{R})$. Then*

$$\hat{\theta}_k^{(\mathrm{DA})} - \theta_k \doteq \hat{\theta}_k^{(\mathrm{SS})} - \theta_k \doteq -\frac{\lambda}{2\pi d_0 p_k \cos\theta_k}\frac{\Im(\boldsymbol{\xi}^T\Delta\boldsymbol{r})}{\boldsymbol{\beta}_k^H\boldsymbol{\beta}_k},$$

where $\doteq$ denotes asymptotic equality and

$$\begin{aligned} &\boldsymbol{\xi}_k = \boldsymbol{F}^T\boldsymbol{\Gamma}^T(\boldsymbol{\beta}_k \otimes \boldsymbol{\alpha}_k), \quad && \boldsymbol{\Gamma} = [\boldsymbol{\Gamma}_{M_{\mathrm{v}}}^T\ \boldsymbol{\Gamma}_{M_{\mathrm{v}}-1}^T\ \cdots \boldsymbol{\Gamma}_1^T]^T, \\ &\boldsymbol{\alpha}_k^T = -\boldsymbol{e}_k^T\boldsymbol{A}_{\mathrm{v}}^\dagger, && \boldsymbol{D} = \mathrm{diag}(0, 1, \ldots, M_{\mathrm{v}}), \\ &\boldsymbol{\beta}_k = \boldsymbol{\Pi}_{\boldsymbol{A}_{\mathrm{v}}}^{\perp}\boldsymbol{D}\boldsymbol{a}_{\mathrm{v}}(\theta_k). \end{aligned}$$

Theorem 2. *The asymptotic MSE expressions of DA-MUSIC and SS-MUSIC have the same form:*

$$\mathbb{E}[(\hat{\theta}_k - \theta_k)^2] \doteq \frac{\lambda^2}{4\pi^2 N d_0^2 p_k^2 \cos^2\theta_k}\frac{\boldsymbol{\xi}_k^H(\boldsymbol{R}\otimes\boldsymbol{R}^T)\boldsymbol{\xi}_k}{\|\boldsymbol{\beta}_k\|_2^4} \tag{5}$$

for $k \in \{1, 2, \ldots, K\}$.

Theorem 1 implies that DA-MUSIC and SS-MUSIC have the same asymptotic estimation error, despite the fact that $\boldsymbol{R}_{\mathrm{v}1}$ is a linear transform of the elements in $\boldsymbol{z}$, and that $\boldsymbol{R}_{\mathrm{v}2}$ is a quadratic transformation of the elements in $\boldsymbol{z}$. Based on Theorem 1, we can derive the asymptotic MSE for both DA-MUSIC and SS-MUSIC, which is presented in Theorem 2.

For brevity, we denote the asymptotic MSE of the k-th DOA as $\epsilon(\theta_k)$. From Theorem 2 we know that $\epsilon(\theta_k)$ is inversely proportional to the number of snapshots and the source power. The term $\cos^2\theta_k$ in the denominator implies that $\epsilon(\theta_k)$ will be large near end-fire regions. Another interesting implication of Theorem 2 is that $\epsilon(\theta_k)$ depends on both the physical array geometry and the virtual array geometry. Even if two arrays share the same virtual array, they may have different $\epsilon(\theta_k)$ because their physical array geometries can be different. An illustrative example is provided in Fig. 1, where we plot the RMSEs for four different nested arrays with (N_1, N_2) set to $(5,6)$, $(2,12)$, $(3,9)$, and $(1,18)$, respectively. It can be easily shown that they share the same virtual ULA. However, as shown in Fig. 1, they exhibit different performances under different signal-to-noise ratio (SNR) settings and different numbers of sources.

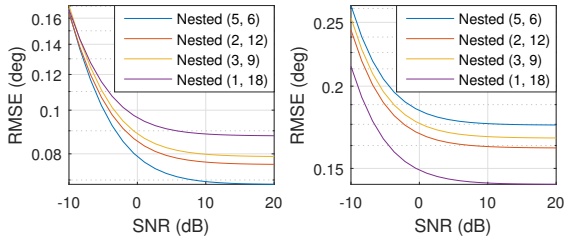

Fig. 1. RMSE vs. SNR for four different nested array configurations. Left: $K = 8$. Right: $K = 20$.

Some interesting properties of $\epsilon(\theta_k)$ in high SNR regions are summarized in Corollary 1, and the special one-source case of Theorem 2 is given in Corollary 2. Specifically, we observe that $\epsilon(\theta_k)$ is strictly greater than zero when the number of sources is greater or equal to the number of sensors. This explains the "saturation" behavior of SS-MUSIC observed in [4] and [3].

Corollary 1. *Assume all sources have the same power p. Let $\mathrm{SNR} = p/\sigma_{\mathrm{n}}^2$ denote the common SNR. Then $\epsilon(\theta_k)$ decreases monotonically as $\bar{p}$ increases, and*

$$\lim_{\mathrm{SNR}\to\infty} \epsilon(\theta_k) = \frac{\lambda^2}{4\pi^2 N d_0^2 p_k^2 \cos^2\theta_k} \frac{\|\boldsymbol{\xi}_k^H(\boldsymbol{A}\otimes\boldsymbol{A}^*)\|_2^2}{\|\boldsymbol{\beta}_k\|_2^4}. \quad (6)$$

Specifically, when $K = 1$, the above expression is exactly zero, and when $K \geq M$ the above expression is strictly greater than zero.

Corollary 2. *Let $K = 1$. Then*

$$\epsilon(\theta) = \frac{36\lambda^2 C}{\pi^2 N M_{\mathrm{v}}^6 d_0^2 p_k^2 \cos^2\theta}, \quad (7)$$

where

$$C = \tilde{\boldsymbol{\xi}}^H(\mathbf{1}_M\mathbf{1}_M^T + \sigma_{\mathrm{n}}^2\boldsymbol{I})\otimes(\mathbf{1}_M\mathbf{1}_M^T + \sigma_{\mathrm{n}}^2\boldsymbol{I})\tilde{\boldsymbol{\xi}}^H, \quad (8)$$

$$\tilde{\boldsymbol{\xi}} = \boldsymbol{F}^T\boldsymbol{\Gamma}^T\Big\{\Big[\Big(\frac{1}{M_{\mathrm{v}}}\boldsymbol{D} - \frac{1}{2}\boldsymbol{I}\Big)\mathbf{1}_{M_{\mathrm{v}}}\Big]\otimes\mathbf{1}_{M_{\mathrm{v}}}\Big\}. \quad (9)$$

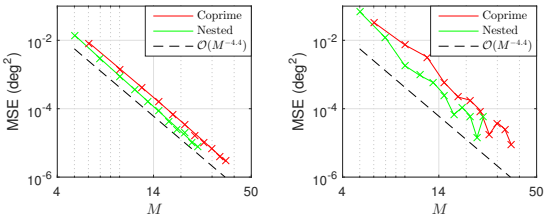

(a) $K = 1$ (b) $K = 3$

Fig. 2. MSE vs. number of sensors. SNR $= 0$dB, and $N = 1000$. The solid lines denote analytical results, while crosses denote numerical results. A dashed black trend line is included for comparison.

Using Theorem 2 and Corollary 2, we can analyze the decreasing rate of $\epsilon(\theta)$ as M goes to infinity. In Fig. 2, we plot $\epsilon(\theta)$ versus the number of sensors, as well as the results obtained from numerical simulations. The co-prime arrays were generated by the co-prime pairs $(m, m+1)$, and the nested arrays were generated by the parameter pairs $(m+1, m)$, where we varied m from 2 to 12. We observe that $\epsilon(\theta)$ decreases at a rate of approximately $\mathcal{O}(M^{-4.4})$ for both array configurations for the one source case. For the multi-source case, we observe that $\epsilon(\theta)$ does not decrease monotonically with respect to M, while approximately following the trend line given by $\mathcal{O}(M^{-4.4})$.

4. THE CRAMÉR-RAO BOUND

The CRB for general sparse linear arrays is given by [12, 13, 15]:

$$\mathrm{CRB}_{\boldsymbol{\theta}} = \frac{1}{N}(\boldsymbol{M}_{\boldsymbol{\theta}}^H\boldsymbol{\Pi}_{\boldsymbol{M}_{\boldsymbol{s}}}^{\perp}\boldsymbol{M}_{\boldsymbol{\theta}})^{-1}, \quad (10)$$

where $\boldsymbol{M}_{\boldsymbol{\theta}} = (\boldsymbol{R}^T\otimes\boldsymbol{R})^{-1/2}\dot{\boldsymbol{A}}_{\mathrm{d}}\boldsymbol{P}$, and $\boldsymbol{M}_{\boldsymbol{s}} = (\boldsymbol{R}^T\otimes\boldsymbol{R})^{-1/2}[\boldsymbol{A}_{\mathrm{d}}\ \boldsymbol{i}]$. Here we define $\dot{\boldsymbol{A}}_{\mathrm{d}} = \dot{\boldsymbol{A}}^*\odot\boldsymbol{A} + \boldsymbol{A}^*\odot\dot{\boldsymbol{A}}$, and $\dot{\boldsymbol{A}} = [\partial\boldsymbol{a}(\theta_1)/\partial\theta_1, \cdots, \partial\boldsymbol{a}(\theta_K)/\partial\theta_K]$. $\boldsymbol{A}_{\mathrm{d}}$ and $\boldsymbol{i}$ follow the same definitions as in (2).

The properties of the CRB (10) in high SNR regions is summarized in Proposition 1 [12]. We observe that when $K \geq M$, the CRB does not go to zero as SNR goes to infinity. This puts a strictly positive lower bound on the MSE of all unbiased estimators.

Proposition 1. *Assume all sources have the same power p, and $[\dot{\boldsymbol{A}}_{\mathrm{d}}\boldsymbol{P}\ \boldsymbol{A}_{\mathrm{d}}\ \boldsymbol{i}]$ is full column rank. Let $\mathrm{SNR} = p/\sigma_{\mathrm{n}}^2$. Then (1) if $K < M$, and $\lim_{\mathrm{SNR}\to\infty}\mathrm{CRB}_{\boldsymbol{\theta}}$ exists, it is zero under mild conditions; (2) if $K \geq M$, and $\lim_{\mathrm{SNR}\to\infty}\mathrm{CRB}_{\boldsymbol{\theta}}$ exists, it is positive definite when $K \geq M$.*

Because both co-prime and nested arrays are constructed from two uniform arrays, we are able to approximate the CRB (10) in case of large M. Our main result on the relationship between the CRB and M for co-prime and nested arrays as M goes to infinity is summarized in Theorem 3. The detailed proof of Theorem 3 will be given in [22].

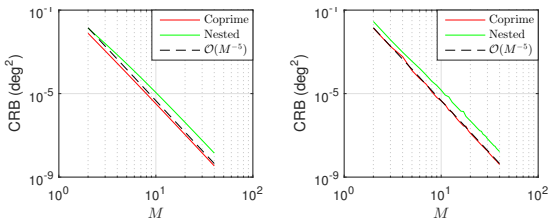

(a) $K = 1$ (b) $K = 3$

Fig. 3. CRB vs. number of sensors. SNR $= 0$dB, and $N = 1000$. A dashed black trend line is included for comparison.

Theorem 3. *Assume that all sources share the same power. For co-prime arrays generated with co-prime pair $(Q, Q+1)$, or nested arrays generated with parameter pair (Q, Q), if we fix $K \ll Q$, then as $Q \to \infty$, the CRB can decrease at a rate of $\mathcal{O}(Q^{-5})$.*

Recall that for ULAs, the CRB decreases at a rate of $\mathcal{O}(M^{-3})$ as $M \to \infty$ [8]. Theorem 3 implies that co-prime and nested arrays can achieve the same performance as ULAs with fewer sensors. As an illustrative example, we plot the CRB versus the number of sensors for co-prime and nested arrays in Fig. 3. We observe that when M is large, the CRB follows the trend line given by $\mathcal{O}(M^{-5})$.

5. APPLICATION TO RESOLUTION ANALYSIS

In this section, we demonstrate the application of Theorem 2 to resolution analysis with numerical examples. We consider the following four array configurations:

- Co-prime (2,3): $[0, 2, 3, 4, 6, 9]d_0$
- MRA: $[0, 1, 2, 6, 9]d_0$
- Nested (1,5): $[0, 1, 3, 5, 7, 9]d_0$
- Nested (4,2): $[0, 1, 2, 3, 4, 9]d_0$

It can be verified that all four arrays have the same aperture.

For two closely spaced sources located at $\theta - \Delta\theta/2$ and $\theta + \Delta\theta/2$, we use the following criterion to analytically determine the resolvability:

$$\sqrt{\epsilon(\theta - \Delta\theta/2)} + \sqrt{\epsilon(\theta - \Delta\theta/2)} \geq \mu\Delta\theta, \qquad (11)$$

where μ is a tunable factor. The resolution limit at θ is obtained by finding the minimum $\Delta\theta$ that satisfies (11). We set $\mu = 1$ and $\theta = 0°$ in the following experiments.

Fig. 4 plots the probability of resolution of different arrays for different numbers of snapshots, with SNR fixed to 0dB. It can be observed that our analytical expression well predicts the resolution limit. It can be also noted that despite having the same aperture, the four different arrays actually exhibit different resolution limits. The nested arrays and the MRA can resolve more closely spaced sources than the co-prime array. Fig. 5 plots the probability of resolution of different arrays for different SNR settings. Again it can be observed that our analytical expression well predicts the resolution limit.

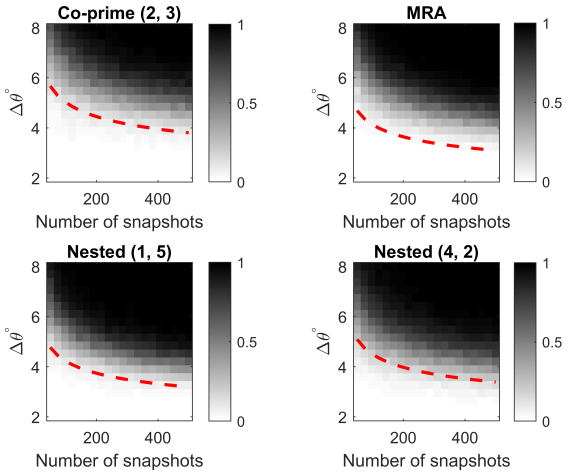

Fig. 4. Resolution probability of different arrays for different N with SNR fixed to 0dB, obtained from 500 trials. The red dashed line is the analytical resolution limit obtained by (11).

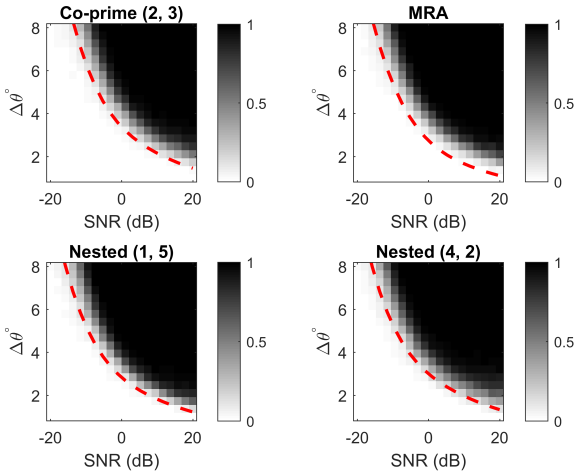

Fig. 5. Resolution probability of different arrays for different SNRs with $N = 1000$, obtained from 500 trials. The red dashed line is the analytical resolution limit obtained by (11).

6. CONCLUSION AND FUTURE WORK

In this paper, we analyzed the asymptotic MSE of DA-MUSIC and SS-MUSIC and the CRB for sparse linear arrays. We showed that when the number of source is greater than the number of sensors, both the MSE and the CRB are strictly non-zero as SNR goes to infinity, which explains the "saturation" behavior of coarray-based MUSIC observed in previous studies. We also showed that for co-prime and nested arrays, the CRB can decrease at a rate of $\mathcal{O}(M^{-5})$. Finally, we demonstrated the application of our asymptotic MSE expression in resolution analysis with numerical examples. In the future, we will examine the possibility of deriving closed form expressions for both the MSE and the CRB in the case of large M. It will also be interesting to incorporate model errors and analyze their influence on the MSE and the CRB.

7. REFERENCES

[1] P. Pal and P. P. Vaidyanathan, "Coprime sampling and the MUSIC algorithm," in *2011 IEEE Digital Signal Processing Workshop and IEEE Signal Processing Education Workshop (DSP/SPE)*, pp. 289–294, Jan. 2011.

[2] Z. Tan, Y. C. Eldar, and A. Nehorai, "Direction of arrival estimation using co-prime arrays: A super resolution viewpoint," *IEEE Transactions on Signal Processing*, vol. 62, pp. 5565–5576, Nov. 2014.

[3] S. Qin, Y. Zhang, and M. Amin, "Generalized coprime array configurations for direction-of-arrival estimation," *IEEE Transactions on Signal Processing*, vol. 63, pp. 1377–1390, Mar. 2015.

[4] P. Pal and P. Vaidyanathan, "Nested arrays: A novel approach to array processing with enhanced degrees of freedom," *IEEE Transactions on Signal Processing*, vol. 58, pp. 4167–4181, Aug. 2010.

[5] K. Han and A. Nehorai, "Wideband Gaussian source processing using a linear nested array," *IEEE Signal Processing Letters*, vol. 20, pp. 1110–1113, Nov. 2013.

[6] K. Han and A. Nehorai, "Nested vector-sensor array processing via tensor modeling," *IEEE Transactions on Signal Processing*, vol. 62, pp. 2542–2553, May 2014.

[7] R. Schmidt, "Multiple emitter location and signal parameter estimation," *IEEE Transactions on Antennas and Propagation*, vol. 34, pp. 276–280, Mar. 1986.

[8] P. Stoica and A. Nehorai, "MUSIC, maximum likelihood, and Cramer-Rao bound," *IEEE Transactions on Acoustics, Speech and Signal Processing*, vol. 37, pp. 720–741, May 1989.

[9] P. Stoica and A. Nehorai, "MUSIC, maximum likelihood, and Cramer-Rao bound: further results and comparisons," *IEEE Transactions on Acoustics, Speech and Signal Processing*, vol. 38, pp. 2140–2150, Dec. 1990.

[10] F. Li, H. Liu, and R. Vaccaro, "Performance analysis for DOA estimation algorithms: unification, simplification, and observations," *IEEE Transactions on Aerospace and Electronic Systems*, vol. 29, pp. 1170–1184, Oct. 1993.

[11] A. Gorokhov, Y. Abramovich, and J. F. Bohme, "Unified analysis of DOA estimation algorithms for covariance matrix transforms," *Signal Processing*, vol. 55, pp. 107–115, Nov. 1996.

[12] M. Wang and A. Nehorai, "Coarrays, MUSIC, and the Cramér Rao bound," *IEEE Transactions on Signal Processing*, vol. 65, pp. 933–946, Feb. 2017.

[13] A. Koochakzadeh and P. Pal, "Cramér Rao bounds for underdetermined source localization," *IEEE Signal Processing Letters*, vol. 23, pp. 919–923, July 2016.

[14] C. L. Liu and P. P. Vaidyanathan, "New cramér-rao bound expressions for coprime and other sparse arrays," in *2016 IEEE Sensor Array and Multichannel Signal Processing Workshop (SAM)*, pp. 1–5, July 2016.

[15] C.-L. Liu and P. P. Vaidyanathan, "Cramér Rao bounds for coprime and other sparse arrays, which find more sources than sensors," *Digital Signal Processing*, pp. 43–61, Feb. 2017.

[16] P. Stoica and A. Nehorai, "Performance study of conditional and unconditional direction-of-arrival estimation," *IEEE Transactions on Acoustics, Speech and Signal Processing*, vol. 38, pp. 1783–1795, Oct. 1990.

[17] G. A. F. Seber, *A matrix handbook for statisticians*. Hoboken, N.J.: Wiley-Interscience, 2008. OCLC: 191879555.

[18] Y. Abramovich, N. Spencer, and A. Gorokhov, "Detection-estimation of more uncorrelated Gaussian sources than sensors in nonuniform linear antenna arrays. I. Fully augmentable arrays," *IEEE Transactions on Signal Processing*, vol. 49, pp. 959–971, May 2001.

[19] C.-L. Liu and P. Vaidyanathan, "Remarks on the spatial smoothing step in coarray MUSIC," *IEEE Signal Processing Letters*, vol. 22, Sept. 2015.

[20] J. H. Wilkinson, *The algebraic eigenvalue problem*. Monographs on numerical analysis, Oxford : Oxford ; New York: Clarendon Press ; Oxford University Press, 1988.

[21] G. W. Stewart, "Error and perturbation bounds for subspaces associated with certain eigenvalue problems," *SIAM Review*, vol. 15, pp. 727–764, Oct. 1973.

[22] M. Wang and A. Nehorai, "Further results on coarrays, MUSIC, and the Cramér-Rao bound," in preparation.